Liquid Crystals
Publication details, including instructions for authors and subscription information:
http://www.informaworld.com/smpp/title~content=t713926090

Surface morphology at nanometer level and optical phase retardation of rubbed alignment films

Y. B. Kim; B. S. Ban

To cite this Article Kim, Y. B. and Ban, B. S.(1999) 'Surface morphology at nanometer level and optical phase retardation of rubbed alignment films', Liquid Crystals, 26: 11, 1579 — 1585
To link to this Article: DOI: 10.1080/026782999203553
URL: http://dx.doi.org/10.1080/026782999203553

Liquid Crystals, 1999, Vol. 26, No. 11, 1579–1585

Surface morphology at nanometer level and optical phase retardation of rubbed alignment films

Y. B. KIM* and B. S. BAN
Liquid Crystal Research Center, Department of Chemistry,
Division of Natural Sciences, Konkuk University, 93-1, Mojindong, Kwanginku,
Seoul 143-701, Korea

(*Received 16 February 1999; accepted 27 May 1999*)

The surface morphology of rubbed polyimide LC aligning films has been studied by scanning force microscopy. We examined three types of alignment film: HT-210, AL-1051 (main chain type) and AL-8044 (side chain type) polyimide surfaces. The rubbed polyimide surfaces show anisotropic alignment of the polymer chain cluster, and a microgroove between the ripple pattern streaks. Also, they are periodically oriented along the rubbing direction. The optical phase retardation of the rubbed surface does not increase with increased cumulative time of rubbing, On the other hand, it increases monotonically with increasing rubbing depth.

1. Introduction

In a liquid crystal (LC) display cell the LC fills the cavity between two surfaces, which act as alignment layers. Owing to the ordered molecular structure of the LC, the effects of the interface can be transferred into the bulk over comparatively large distances, influencing its structure and electro-optical properties. Thus, it has become of interest to investigate the properties of the alignment layer and possibly the first few molecular monolayers of LC at the interface.

It is well known that LC molecules may be aligned on a rubbed polyimide surface or on an elongated polymer film [1]. Although many theoretical and experimental studies have been made on this subject, the actual alignment mechanism has not been clarified [2–10].

One possibility is that the alignment is induced by grooves or scratches mechanically formed on the polymer surface by the rubbing process [2, 3]. An alternative concept is that alignment acts through the orientation of polymer molecules [6, 7]. Obviously, the surface morphology at the nanometer level is important for understanding the alignment mechanism of LC molecules. On these very flat surfaces it is difficult to use ordinary electron microscopy due to the low height resolution. Instead, scanning tunnelling microscopy (STM) has been used to image rubbed polymer surfaces [11–13]. However, STM requires conducting samples, and the polymers must be coated with a conductive layer. As is well known, the technique of scanning force microscopy (SFM), which does not require the sample to be conducting, is better suited for investigation of both thin films and the surfaces of bulk organic materials [14, 15]. This technique generates images with nanometer resolution by raster scanning a sharp tip over the surface at constant tip–sample force [11]. In our opinion SFM already gives much information on the aligning polymer layers used in LC cell fabrication.

SFM studies of rubbed polymers have shown that grooves are present on the surface [13, 16–21]. In this work, we will describe the surface morphology at nanometer level and the optical phase retardation of rubbed alignment films as a function of the rubbing strength.

2. Experimental

Our experiments were performed using three samples of polyimide alignment material; HT-210 (Toray Industries), AL-1051 and AL-8044 (JSR Co.). The polyimide solution was spin coated on ITO coated glass, the solvent evaporated at 80°C for 30 min; curing was carried out at 180 or 300°C, in each case for 1 h. The approximate thickness of the resulting polyimide films was about 800 ± 50 Å. Rubbing was performed by pressing the sample onto nylon velvet (subfibre diameter: 2 μm, length: 1.8 mm) wound on a rubbing roller; the roller was then moved in one direction over the sample for a fixed distance at a known transverse speed and rotation velocity of the roller.

The rubbing strength RS was calculated using the empirical expression:

$$RS = \gamma L = \gamma N l \left(1 + \frac{2\pi r n}{60 v}\right) \qquad (1)$$

---

*Author for correspondence;
e-mail: yongkim@kkucc.konkuk.ac.kr

Journal of Liquid Crystals ISSN 0267-8292 print/ISSN 1366-5855 online
http://www.tandf.co.uk/JNLS/lct.htm
http://www.taylorandfrancis.com/JNLS/lct.htm

where γ is a characteristic parameter of the rubbing process which includes the rubbing pressure, the fibre density of the rubbing material, the coefficient of friction, etc. L is the total length of the rubbing fibre contacting a given point of the substrate. N is the number of rubbing actions, l is the contact length (mm) on the circumference of the rubbing roller, n is the number of revolutions per minute (rpm) of the roller, r is the radius (m) and v is the speed (m sec^{-1}) of the substrate stage. In equation (1), γ is difficult to define but L can be defined definitely as the rubbing parameter for the examination of the effects of 'rubbing time' and rubbing depth. The 'rubbing time' is the cumulative number of rubbing actions. The rubbing depth is the depth of impression of the rubbing fibre on a certain point of the sample surface.

We assumed that the friction coefficient had the same value for all tested polyimide materials, using the same rubbing fibre and the same rubbing pressure. Thus, the rubbing strength was proportional only to the rubbing time N. On the other hand, with the rubbing time kept constant, the rubbing strength was proportional only to the contact length l. We observed a deformation of surface morphology for rubbing times from 1 to 8 and for rubbing depths from 0.05 to 0.7 mm.

The SFM measurements were performed using a commercial apparatus (Universal System, Park Science Instruments, CA) operated in the contact mode with constant-force. Standard Si_3N_4 SFM tips, with a force constant of 0.032 N m^{-1}, were used. The tip–sample force in all images was about 10 nN and the scan frequency was in the range 0.5–1 Hz. The images were tilt corrected and low-pass filtered.

The optical phase retardation was measured using an ADR-500xy (ORC Manufacturing Co.) system, see figure 1. No difference in retardation was found between uncoated and coated glass samples. The uncoated glass samples exhibited their own value as 4.3×10^{-4} cycles approximately. First, a measurement of retardation of the unrubbed polyimide coated sample was made. The sample was then rubbed under the experimental conditions and the optical phase retardation and SFM image again measured. This process was continued, yielding a series of values.

3. Results and discussion

The SFM images of a polyimide (HT-210) film are shown in figure 2. The structures of the polyimide surface are drastically changed during the rubbing process. The unrubbed polyimide surface image appeared as a stone surface (figures 2A and 3). Various size spherical clusters of polyimide chain are randomly distributed, as illustrated in figure 3.

Such images are not surprising since the polymer chain forms a spherical cluster in the solvent. When the polymer solution is deposited on the substrate, and the solvent evaporated, the polymer chain cluster covers the surface like separating islands of deformed spherical shape. Their density depends on the polymer concentration in the solvent. The rubbed surface is dramatically changed to a very flat surface having a line pattern oriented along the rubbing direction (figure 2B). In figure 2C we show a higher resolution image composed of several segments of 1 × 1 μm² scan size image obtained from the 4 × 4 μm² area shown in figure 2B.

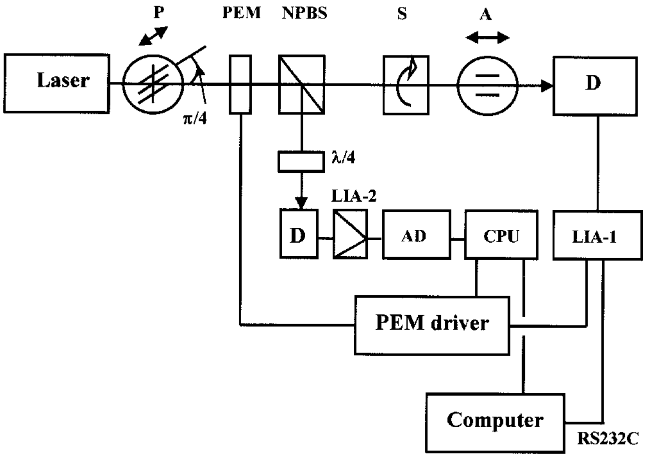

Figure 1. The system set-up for automatic double retardation measurement of polyimide alignment. Laser = He-Ne laser, P = polarizer, PEM = photo-elastic modulator, NPBS = non-polarized beam splitter (mirror), S = sample, A = analyser, D = photo-detector, LIA-1 = D.C. amplifier, LIA-2 = A.C. amplifier, CPU = computer, AD = A/D converter.

The rubbing raised a long line of polymer chain clusters, periodically aligned and standing side by side along the rubbing direction. Figures 4 and 5 show higher resolution images of the region A and the thicker lines shown in figure 2C. The streaks of the ripple pattern stand periodically side by side along the rubbing direction. Long microgrooves are observed between the ripple patterns. Small microgrooves are observed in the ripple pattern, aligned along the rubbing direction (figure 4). A higher resolution image, 0.53 × 0.53 μm² scan size, of the thicker line shown in figure 2C is shown in figure 5. Rubbing elongated the polymer chain spherical cluster and aligned it to the rubbing direction as shown in figures 4 and 5. The row of ellipsoidal clusters stood side by side along the rubbing direction. Here, we suggest referring to the ellipsoidal cluster line as 'cluster chain'.

The geometry of a deformation formed by rubbing is illustrated in figure 6. The diameter of a rubbing fibre is a approximately 2 μm, as shown in figure 6(*a*); these fibres are contacted with polyimide surface as shown in figures 6(*b*) and 6(*c*). The polyimide surface is rubbed by the unidirectional motion of fibre in contact with the

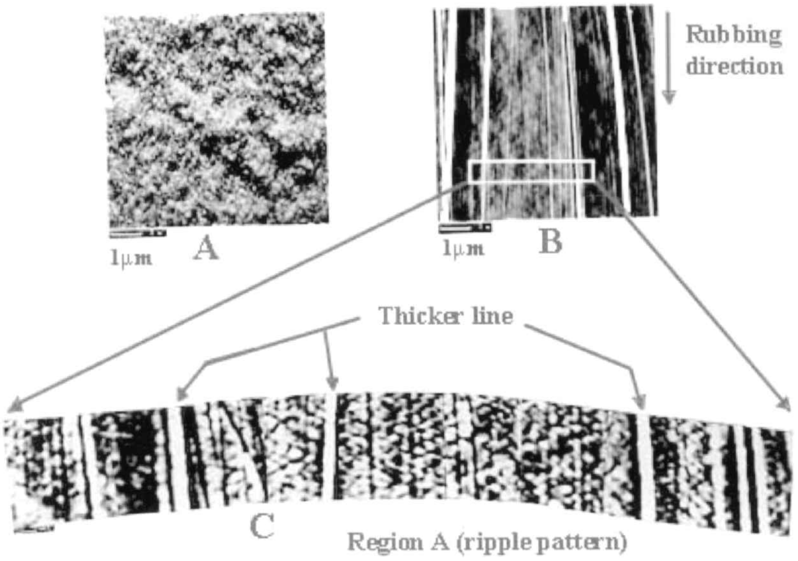

Figure 2. SFM images of a film of polyimide HT-210. A: unrubbed surface (scan size $8\times 8\,\mu m^2$, grey scale 1.6 nm), B: rubbed surface (scan size $8\times 8\,\mu m^2$, grey scale 1.5 nm). C: higher resolution image of rectangular area in B.

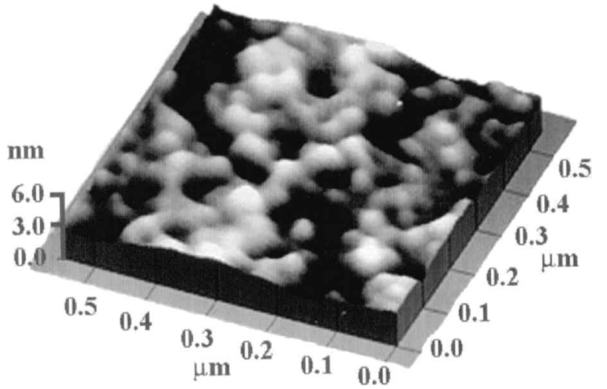

Figure 3. SFM images of an unrubbed film of polyimide HT-210. The cluster varies in size and is randomly distributed (grey scale 1.6 nm).

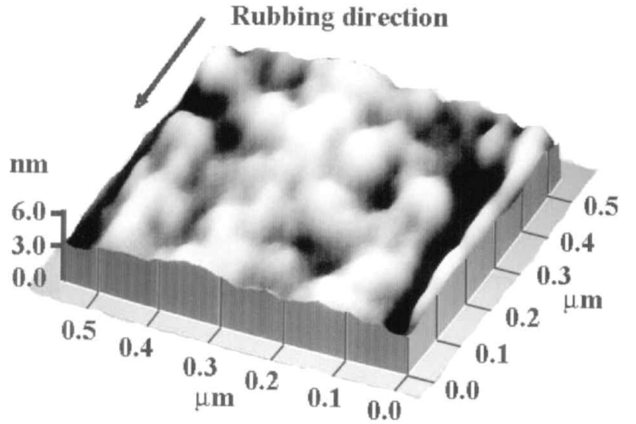

Figure 5. Higher resolution image of the thicker line shown in figure 2C (scan size $0.53\times 0.53\,\mu m^2$).

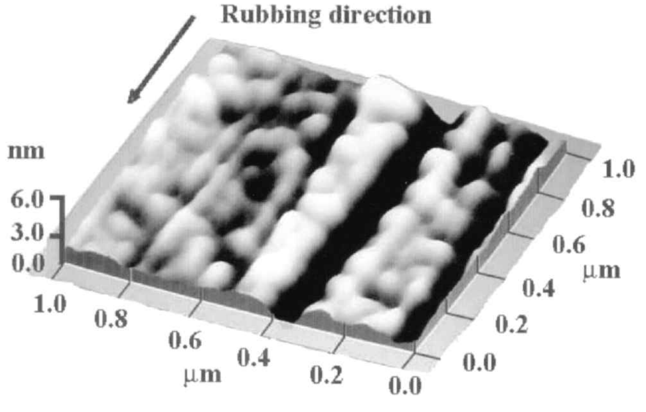

Figure 4. SFM image of the rubbed surface of HT-210 showing grooves (scan size $1\times 1\,\mu m^2$, grey scale 15 nm).

surface. The extent of contact caused by the rubbing pressure between the fibre and the polyimide surface, while substantially less than the fibre diameter, can reasonably be expected to be substantially broader than the film thickness. Hence, during the rubbing the polyimide film is caught between two broad planes, one stationary (substrate) and the other moving (the fibre contact area).

It is important to understand the elongation and alignment mechanism of the polyimide chain caused by the rubbing process. We suggest that two factors act on the polyimide surface: these are local heating, and a simultaneous shearing force. If the friction exerted by the fibre on the contact area is great enough, a permanent shearing deformation can be generated, as shown in figure 6(*c*). Whatever the precise form of the shearing deformation produced by the rubbing process, there will always be a residual inclination of the elongation axis of the polymer at the surface [7]. The sense of inclination is the same as the sense of tilt of the orientation axis of the polymer, as shown in figure 6(*b*). Both factors have

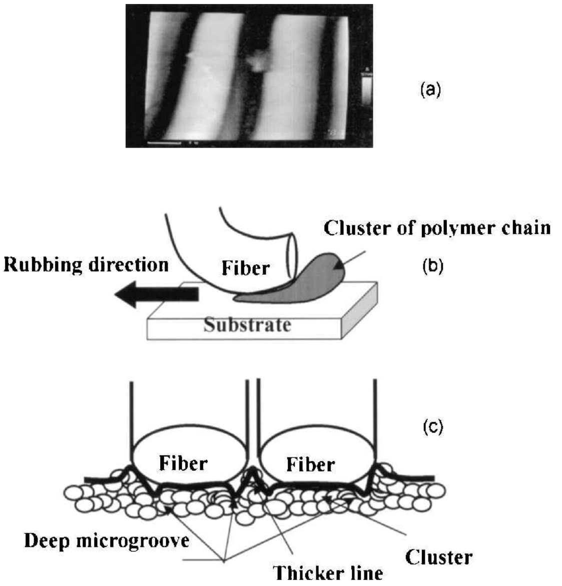

Figure 6. (a) SFM image of rubbing fibre; (*b*) and (*c*) the side and cross section view, respectively, of a polyimide film in contact with rubbing fibres.

contributed to elongate the polyimide chain cluster and to align the ellipsoidal clusters along the rubbing direction. In this way, the axis of elongation will be nearly parallel to the rubbing direction and the polymer surface. Thus, through the action of shearing, the polyimide surface will be deformed much as if it had first been aligned and the polyimide chain cluster elongated by cold drawing, and then placed upon the substrate as shown in figures 4 and 5.

The overall tendency is that the spherical clusters become elongated in the rubbing direction, and the shearing deformation always produces inclination of the elongation axis of the polymer chain cluster at the surface as shown in figure 6 (*b*). Figures 5 and 6 (*c*) show the coalescence of neighbouring cluster chains between the rubbing fibres; they are then changed into thicker bundles, consisting of two or more, due to the local heating and simultaneous shearing force during the rubbing process.

In comparative experiments on main chain and side chain type polyimides, we have observed a variation of the surface morphology as a function of the rubbing times and depths. The polyimide surface structures were slightly changed with lower rubbing depth, but greatly changed at deeper rubbing depth as illustrated in figure 7. That is, as the rubbing depth is increased from 0.05 to 0.7 mm at constant rubbing times, the degree of orientation of chain clusters in the polyimide surface is increased for both types of polyimide.

When the rubbing depth is changed from 0.3 to 0.7 mm, the anisotropic alignment of clusters can be clearly noticed. It is understandable if one considers that the contact areas between the rubbing fibre and the polymer surface are sufficiently larger to deform the polymer surface. For a deeper rubbing depth of 0.7 mm in the side chain type polyimide surface, the neighbouring chains seem to coalesce forming thicker bundles of chains due to local heating and simultaneous shearing force. Also, it is observed that the row-like cluster chain and the microgrooves are periodically aligned along the rubbing direction.

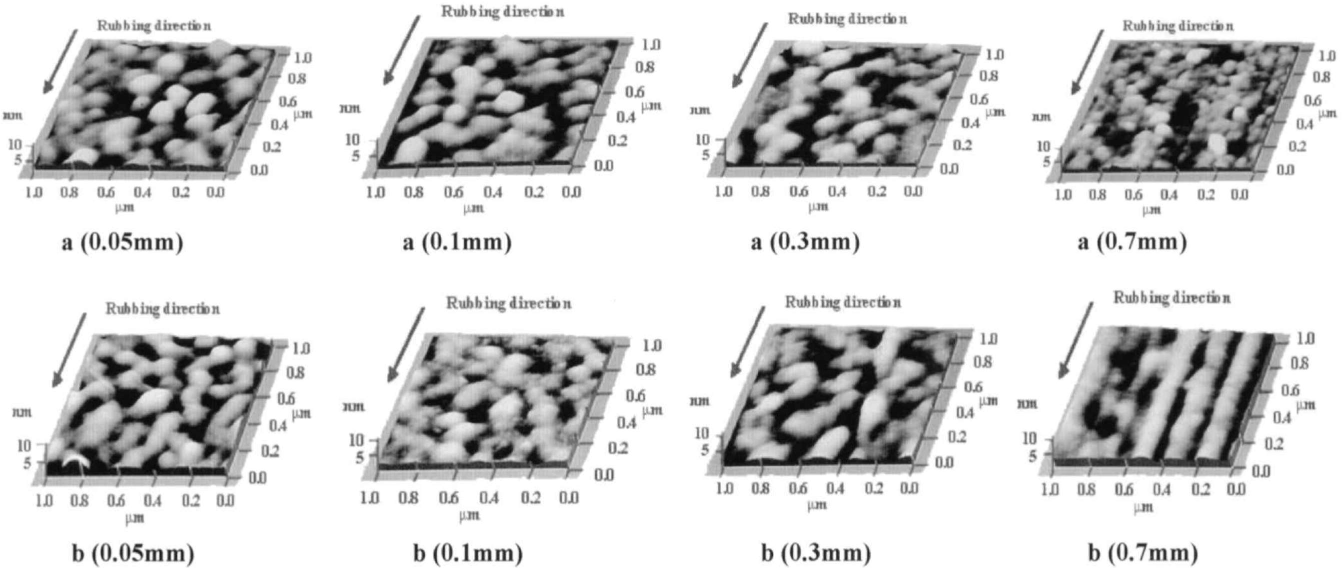

a (0.05mm) a (0.1mm) a (0.3mm) a (0.7mm)

b (0.05mm) b (0.1mm) b (0.3mm) b (0.7mm)

Figure 7. SFM images exhibiting the influence of increasing rubbing depth at a constant cumulative rubbing time (1 rubbing action) and scan size $1 \times 1\ \mu m^2$. (*a*) AL-1051, (*b*) AL-8044; the rubbing depths are given in parentheses.

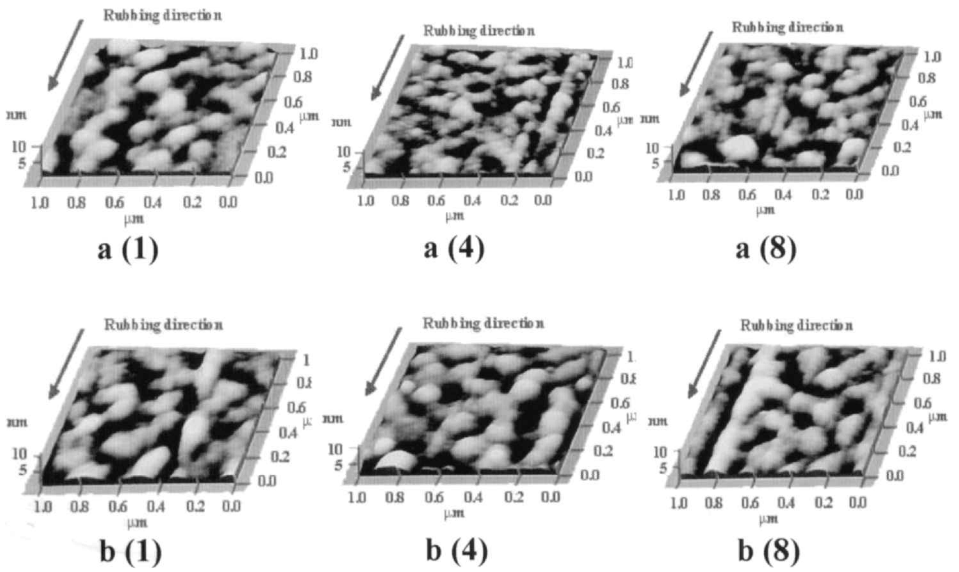

Figure 8. SFM images showing the influence of increasing rubbing times at a constant rubbing depth of 0.3 mm and scan size $1 \times 1\,\mu m^2$. (*a*) AL-1051, (*b*) AL-8044; the rubbing times (number of rubbing actions) are given in parentheses.

The cluster size of the side chain type polyimide is larger than that of the main chain type. The surface morphology of the side chain type undergoes a greater change than that of the main chain type of the polyimide. This may be due to the size and the structure differences in the polyimide monomers.

On the other hand, once an oriented string structure is obtained with a strong rubbing strength, no great changes in the surface morphology are visible, even when the rubbing times are increased from 1 to 8 at a constant rubbing depth of 0.3 mm, as illustrated in figure 8. At a first rubbing with a rubbing depth of 0.3 mm, most of the cluster on the rubbed surface was oriented in the rubbing direction. As the rubbing process continued, the surface morphology showed no remarkable variation.

In general, polymer chain orientation is known to induce birefringence. Therefore, the measurement of retardation is a useful method for the detection of chain orientation induced by the rubbing process. The observed rubbing-induced retardation for AL-1051 (main chain type) and AL-8044 (side chain type) polyimide surface, plotted as a function of the cumulative rubbing times, is shown in figure 9.

As shown in figure 9, the observed retardation induced by the first rubbing is 0.42 nm for AL-8044 and 0.53 nm for AL-1051. The retardation is slightly increased with cumulative rubbing times from 1 to 8 at a constant rubbing depth of 0.3 mm. The larger rubbing depth produced a strong shear force and higher local heating in the contact area between the rubbing fibre and the virgin surface of the polyimide. Therefore, the first rubbing produces mainly a higher orientation of polymer cluster chain and a large shearing deformation of the polymer surface. It was found that even if cumulative rubbing process are repeated with the same rubbing depth on a surface after its first rubbing, the retardation induced by the polymer chain orientation does not show a large increment. This is due to a decrease in the rubbing pressure in the fibre contact area on a first-rubbed surface. Thus, the rubbed surface will experience a small shearing force, and the friction energy in the fibre contact area is decreased.

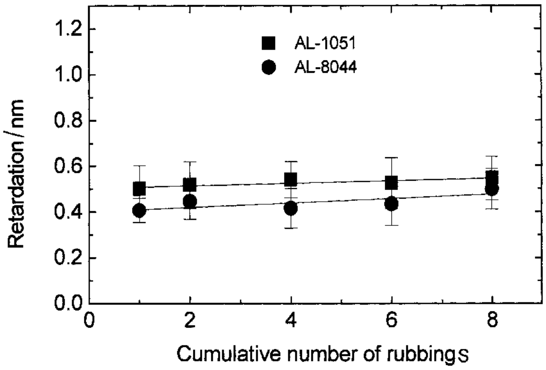

Figure 9. Optical retardation of the rubbed polyimide films as a function of cumulative number of rubbing actions.

Figure 10 shows the effect on retardation of increasing rubbing depths. The retardation was monotonically increased from about 0.1 to 1.0 nm for AL-1051 and 0.1 to 0.8 nm for AL-8044, without saturation. The rubbing pressure created a contact area between fibre and polyimide surface, which increased with the increasing

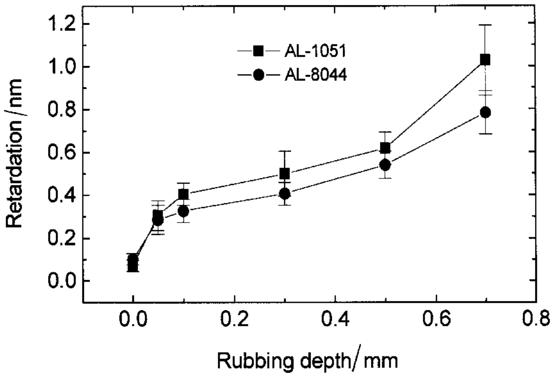

Figure 10. Optical retardation of the rubbed polyimide films as a function of rubbing depth.

rubbing depth. The retardation of the rubbed surface was caused by the anisotropic alignment of clusters, elongated and oriented by the shearing force and the friction energy induced by the rubbing. The reorientation of AL-1051 was greater than that of AL-8044; this may be due to the steric hindrance effect of the polyimide side chain.

Two kinds of the orientation process induced by the rubbing must be considered. The first is the orientation of the polymer chain cluster, the second is the elongation of the polymer chain in clusters along the rubbing direction. Steric hindrance to the anisotropic elongation of a polymer chain cluster is understandable if one considers that the polymer chain distribution is different from the chain structure of the alignment material. Thus, the main chain type receives no steric hindrance from the anisotropic polymer chain orientation, unlike the side chain type at the same rubbing pressure.

We will describe the mechanism of rubbing-induced polymer chain orientation, using the hypothetical picture shown in figure 11. As rubbing proceeds, the clusters in the contact areas are elongated and aligned along the rubbing direction. Anisotropic cluster elongation then creates retardation of the polymer film; micro-grooves are also formed. At first, the contact areas encounter only virgin surface, and the alignment cluster density increases as the area that has been rubbed increases. But as the total rubbing time accumulates, the streaks begin to overlap, and the anisotropy elongation and alignment density of clusters show no further increase (figures 8 and 9). Assuming that most of the deformation, caused by the shearing force and frictional heat at contact areas, occurs on first contact, it is then clear that the observed retardation will increase rapidly, as more and more of the surface is rubbed (figures 7 and 10).

4. Conclusion

Surface images of unrubbed and rubbed polyimide films have been observed directly using SFM. The unrubbed polyimide surface consists of randomly distributed clusters of polymer chain, whose sizes are much greater than an individual polymer molecule. Rubbing produced anisotropic alignment of polymer chains, and microgrooves which were markedly aligned along the rubbing direction. Direct observation of the optical retardation of rubbed surfaces was made. The rubbing process, led to retardation caused by the anisotropic alignment and the orientation of polymer chain clusters. This is due to shearing deformation from frictional heat produced by the rubbing. At higher rubbing depth, cumulative rubbing actions do not lead to anisotropy elongation and the alignment density of clusters does not increase. On the other hand, these properties increase monotonically with increasing rubbing depth.

This work was supported by Korea Science and Engineering Foundation (KSEF) under contract #95-0300-13-01-3.

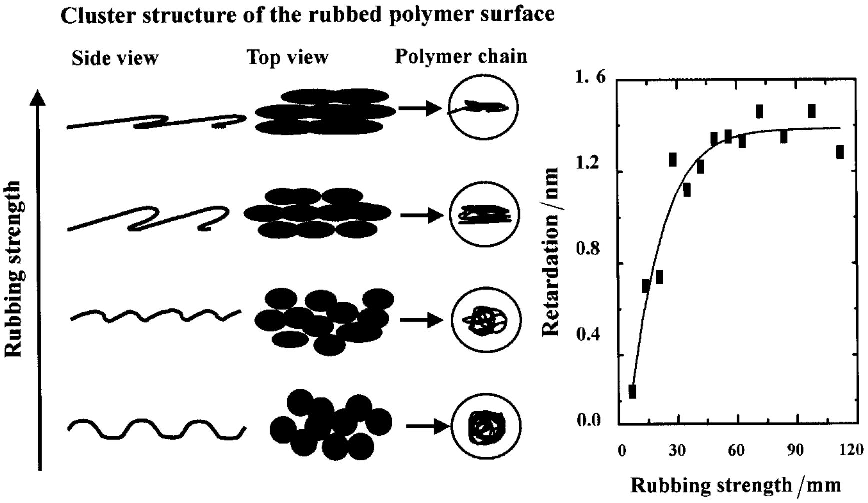

Figure 11. Expected realignment of the polyimide film surface in relation to the rubbing strength.

References

[1] Cognard, J., 1982, *Mol. Cryst. liq. Cryst., Suppl.*, **1,** 1.
[2] Berreman, D. W., 1972, *Phy. Rev. Lett.*, **28,** 1683.
[3] Berreman, D. W., 1973, *Mol. Cryst. liq. Cryst.*, **23,** 215.
[4] Okano, K., 1982, *Jpn. J. appl. Phys.*, **22,** L343.
[5] Okano, K., Matsuura, N., and Kobayashi, S., 1982, *Jpn. J. appl. Phys.*, **21,** L109.
[6] Castello, J. A., 1983, *Mol. Cryst. liq. Cryst.*, **94,** 33.
[7] Geary, J. A., Goodby, J. W., Kmetz, A. R., and Patel, J. S., 1987, *J. appl. Phys.*, **2,** 4100.
[8] Sato, Y., Sato, K., and Uchida, T., 1992, *Jpn. J. appl. Phys.*, **31,** L579.
[9] Han, K. Y., Vetter, P., and Uchida, T., 1993, *Jpn. J. appl. Phys.*, **32,** L1242.
[10] Lee, E. S., Vetter, P., Miyashita, T., and Uchida, T., 1993, *Jpn. J. appl. Phys.*, **32,** L1339.
[11] Rinnin, G., Fohrer, H., Gerber, C., and Weibel, E., 1982, *Phys. Rev. Lett.*, **49,** 57.
[12] Nejoh. H., 1991, *Surf. Sci.*, **256,** 94.
[13] Suzuki, M., Maruilo, T., Yamamoto, F., and Nagai, K., 1990, *J. vac. Sci, Technol.*, **A8,** 631.
[14] Birinig, G., Gerber, C., and Quate, C. F., 1986, *Phys. Rev. Lett.*, **56,** 930.
[15] Liansinii, P. K., Elings, V. B., Bracker, C. E., and Marli, O., 1989, *Science*, **242,** 209.
[16] Kim, Y. B., Kim, H. S., Choi, J. S., Matuszcsyk, M., Olin, H., Buivydas, M., and Rudquist, P., 1995, *Mol. Cryst. Liq. Cryst.*, **262,** 89.
[17] Kim, Y. B., Olin, H., Park, S. Y., Choi, J. W., Komitov, L., Matuszcsyk, M., and Largerwall, S. T., 1995, *J. Appl. Phys. Lett.*, **66,** 2218.
[18] Kim, Y. B., Ban, B. S., and Olin, H., 1996, in *Proceedings of the 16th International Liquid Crystal Conference*, P-111.
[19] Ban, B. S., Jeon, Y. J., and Kim, Y. B., 1996, in *Program and Abstract of The 50th Anniversary Conference and 77th Congress of the Korean Chemical Society*, p. 181.
[20] Matuszcsyk, M., Matuszczyk, T., Largerwall, S. T., Kim, Y. B., Wnek, M., and Maltese, P., 1996, *Ferroelectrics*, **178,** 41
[21] Zhu, Y. M., Wang, L., Lu, Z. H., Wei, Y., Hen, X. X., and Tang, J. H., 1994, *Appl. Phys. Lett.*, **65,** 49.